

# Nonlinear Observer on $SO(3)$ for Attitude Estimation on Rotating Earth Using Single Vector Measurements

Joel Reis<sup>1b</sup>, Pedro Batista<sup>1b</sup>, *Senior Member, IEEE*, Paulo Oliveira<sup>1b</sup>, *Senior Member, IEEE*, and Carlos Silvestre<sup>1b</sup>, *Member, IEEE*

**Abstract**—This letter presents a novel attitude estimation solution, built on  $SO(3)$ , that resorts to single measurements of a constant inertial vector, in addition to angular velocity readings provided by a set of three high-grade fiber optic rate gyros, which are assumed to be sensitive to the angular motion of the Earth. This approach contrasts with typical attitude solutions that require either a single but time-varying inertial vector, or measurements of two non-collinear inertial vectors. The designed nonlinear observer features only one tuning scalar parameter that, in view of the region of convergence of the rotation matrix error, is shown to render the proposed solution almost globally asymptotically stable. Extensive simulation results with realistic noise, including Monte Carlo, are presented that allow to assess the achievable performance.

**Index Terms**—Attitude observer, single body-vector, spherical rotating earth, topological constraints, almost global stability.

## I. INTRODUCTION

THE CEASELESS and widespread developments of robotic platforms have created, over the past years, an increasing demand for more accurate and robust algorithms, particularly those concerned with attitude estimation, which play a key role, for instance, in the design of advanced control strategies for autonomous vehicles. Since the release of Wahba's seminal work [1], which proposed, for the first time, an optimality based approach, increasingly many contributions to the problem of attitude determination have been made that broadened the extent of practical applications, including, nowadays, spacecraft, ballistic missiles, and underwater vessels, to name just a few. Universal progresses made in terms of low-cost sensors, such as strapdown accelerometers and gyroscopes, further drew the attention of the scientific community to the problem, see [2], [3] and references therein.

According to the survey in [4], the strategies for addressing attitude determination rely commonly on variations of the celebrated extended Kalman filter (EKF), but its sensitivity to initial conditions, which can sometimes raise divergence issues, prompted a search for other types of observers. Despite these drawbacks, the EKF remains an actively researched field. In particular, Barrau and Bonnabel [5] have recently shown that the invariant EKF, when used as a deterministic observer for a novel class of problems on Lie groups, is shown to possess theoretical stability guarantees under the simple and natural hypotheses of the linear case.

Overall, the solutions found in the literature can be typically divided into two sets: one set consisting of strategies complying with the topological constraints of  $SO(3)$ , where the attitude evolves in the form of a rotation matrix, see [6]–[8]; and, another set featuring solutions that, despite neglecting the properties of the 2-sphere manifold, offer guarantees of stability and asymptotic convergence, see, for instance [9] and [10]. The major pitfall inherent to the solutions of the first set lies in the fact that a continuous time dynamical system evolving

Manuscript received September 3, 2018; revised November 19, 2018; accepted December 5, 2018. Date of publication December 13, 2018; date of current version December 27, 2018. This work was supported in part by the Macao Science and Technology Development Fund under Grant FDCT/026/2017/A1, in part by the University of Macau, Macau, China, under Project MYRG2018-00198-FST, and in part by the Portuguese Fundação para a Ciência e a Tecnologia (FCT) through the Institute for Systems and Robotics under Laboratory for Robotics and Engineering Systems under Grant UID/EEA/50009/2013, through the Institute for Mechanical Engineering under Associated Laboratory for Energy, Transports and Aeronautics under Grant UID/EMS/50022/2013, and through the FCT project DECENTER funded by the Lisboa 2020 and PIDDAC programs under Grant LISBOA-01-0145-FEDER-029605. Recommended by Senior Editor M. Guay. (Corresponding author: Joel Reis.)

J. Reis is with the Department of Electrical and Computer Engineering, Faculty of Science and Technology, University of Macau, Macau, China (e-mail: joelreis@um.edu.mo).

P. Batista is with the Institute for Systems and Robotics, Instituto Superior Técnico, Universidade de Lisboa, 1049-001 Lisbon, Portugal (e-mail: pbatista@isr.tecnico.ulisboa.pt).

P. Oliveira is with the Institute for Systems and Robotics, Instituto Superior Técnico, Universidade de Lisboa, 1049-001 Lisbon, Portugal, and also with the LAETA—Associated Laboratory for Energy, Transports and Aeronautics, IDMEC—Institute of Mechanical Engineering, Instituto Superior Técnico, Universidade de Lisboa, 1049-001 Lisbon, Portugal (e-mail: paulo.j.oliveira@tecnico.ulisboa.pt).

C. Silvestre is with the Department of Electrical and Computer Engineering, Faculty of Science and Technology, University of Macau, Macau, China, on leave from the Instituto Superior Técnico, Universidade de Lisboa, 1049-001 Lisbon, Portugal (e-mail: csilvestre@um.edu.mo).

Digital Object Identifier 10.1109/LCSYS.2018.2886740

on a state space that has the structure of a vector bundle on a compact manifold possesses no globally asymptotically stable equilibrium [11]. This, however, is not a deterrent to practical implementations of these algorithms. Kalabić *et al.* [12] propose a model predictive control law that is able to achieve global asymptotic stability on  $SO(3)$  because the law may be discontinuous. Furthermore, the recent work in [13] also managed to circumvent the topological constraints of  $SO(3)$  and achieve global stability by adopting a hybrid solution that makes use of potential functions with specific properties.

In this letter, a nonlinear attitude observer is proposed where only one vector measurement is employed, an approach also considered in both [9] and [14]. But, whereas in these two works the inertial counterpart of the vector measurement is time-varying, herein the problem is confined to the aggravated case where it is constant. Indeed, in [14] an observability condition is imposed that requires a persistent change of the reference vector measured in the inertial frame. Moreover, in this letter the Earth's rotation is taken into account in the design of the observer, a trait also pursued in [15], as well as in past work by the authors, see [10]. In contrast to the latter, the technique proposed in this letter is computationally less complex and, instead of multiple tuning parameters, features just one scalar gain that is shown to render the nonlinear attitude observer almost globally asymptotically stable (AGAS). More importantly, while with two vectors one can obtain a good initial estimate of the attitude, in this case that is not possible (the initial error can be very large), hence the significance of AGAS guarantees.

Most noticeably, these features preclude the need for a gyrocompass, a device which is nonetheless a feat of engineering, capable of indicating the true north while being unaffected by the magnetic field. While some past gyrocompass-based solutions had to remain relatively insensitive to pitch and roll movements in order to obtain accurate attitude information [16], recent strap-down technological and algorithmic developments have managed to overcome that caveat, as it is the case of the compact iXblue Octans Survey-Grade Surface Gyrocompass. However, the observer developed in this letter does not require an initial stillness period while finding north and, since it dynamically estimates the rotation matrix, as opposed to direct integration of measurements, drift problems do not occur over time.

In previous work by Reis *et al.* [17], the observer was shown to be locally exponentially stable, whereas herein it is shown to be AGAS, which is a stronger theoretical result in terms of observer design. Moreover, in [17] only a sketch of the performance was presented. In this letter, an extensive Monte Carlo analysis is carried out to illustrate the achievable performance for all possible initial conditions in the presence of realistic noise corresponding to the sensor's worst-case specifications.

The rest of this letter is organized as follows: in Section II, an overview of the problem statement is presented followed by steps leading to the proposed attitude observer. In Section III, the main result of this letter is developed, where the attitude observer is shown to be AGAS. Section IV features simulation results that allow to assess the achievable performance of

the nonlinear attitude estimation solution. Finally, Section V elaborates upon a few conclusions and comments on this letter.

## A. Notation

Throughout this letter, a bold symbol stands for a multidimensional variable, the symbol  $\mathbf{0}$  denotes a matrix of zeros and  $\mathbf{I}$  an identity matrix, both of appropriate dimensions. The set of unit vectors on  $\mathbb{R}^3$  is denoted by  $S(2)$ . The special orthogonal group is denoted by  $SO(3) := \{\mathbf{X} \in \mathbb{R}^{3 \times 3} : \mathbf{X}\mathbf{X}^T = \mathbf{X}^T\mathbf{X} = \mathbf{I} \wedge \det(\mathbf{X}) = 1\}$ . The skew-symmetric matrix of a vector  $\mathbf{a} \in \mathbb{R}^3$  is defined as  $\mathbf{S}(\mathbf{a})$ , such that given another vector  $\mathbf{b} \in \mathbb{R}^3$  one has (the cross-product)  $\mathbf{a} \times \mathbf{b} = \mathbf{S}(\mathbf{a})\mathbf{b}$ . Finally, for convenience, the transpose operator is denoted by the superscript  $(\cdot)^T$  and the trace function by  $\text{tr}(\cdot)$ .

## II. DESIGN OF ATTITUDE OBSERVER

### A. Problem Statement

Consider a robotic platform with a body-fixed frame associated to it. Suppose this platform is equipped with the commercial off-the-shelf high performance Fiber Optic Gyro (FOG) inertial measurement unit (IMU) KVH DSP-1775, which provides measurements of angular velocity in addition to either acceleration or magnetometer readings. The magnetic vector field is an apt example of a body measurement that has a constant inertial counterpart, which herein is assumed known. Nevertheless, as convincingly argued in [6], since the gravitational field is much larger than the body acceleration for typical maneuvers, one can also assume the accelerometer measurements are constant when expressed in the inertial frame.

Within the scope of this letter, the IMU is assumed to have been pre-calibrated, whereby its readings can be assumed unbiased and free of sensor non-idealities.

Since the aforementioned FOG IMU is sensitive to the Earth's rotation, the angular velocity readings feature implicit measurements of said rotational velocity. Overall, all measurements with respect to the body-fixed frame can be expressed in a given inertial frame by means of an unknown rotation matrix. Hence, the aim of this letter is to present an observer for the rotation matrix based on angular velocity readings and on body measurements of a known constant inertial vector. As opposed to previous work by the authors, and to most solutions found in the literature, the observer presented in this letter resorts to measurements of a single reference vector, in addition to implicit measurements of the Earth's angular velocity, while simultaneously preserving topological properties.

### B. Observer for the Orientation Matrix

Let  $\mathbf{R}(t) \in SO(3)$  denote the rotation matrix from a body-fixed frame  $\{B\}$  to a local inertial coordinate reference frame  $\{I\}$ . The evolution in time of this rotation matrix obeys

$$\dot{\mathbf{R}}(t) = \mathbf{R}(t)\mathbf{S}[\boldsymbol{\omega}(t)], \quad (1)$$

where  $\boldsymbol{\omega}(t) \in \mathbb{R}^3$  is the angular velocity of  $\{B\}$  with respect to  $\{I\}$ , expressed in  $\{B\}$ . The measurements  $\boldsymbol{\omega}_m(t) \in \mathbb{R}^3$  from a

set of three high-grade, orthogonally mounted rate gyros are given by

$$\boldsymbol{\omega}_m(t) = \boldsymbol{\omega}(t) + \boldsymbol{\omega}_E(t), \quad (2)$$

where  $\boldsymbol{\omega}_E(t) \in \mathbb{R}^3$  is the angular velocity of the Earth around its own axis, expressed in  $\{B\}$ . In turn, let the vector measurements provided by the second sensor be denoted as  $\mathbf{m}(t) \in \mathbb{R}^3$ . These, when expressed in inertial coordinates, are assumed to be constant. Hence, let  ${}^I\boldsymbol{\omega}_E$  and  ${}^I\mathbf{m}$  be the inertial vector counterparts corresponding to  $\boldsymbol{\omega}_E(t)$  and  $\mathbf{m}(t)$ , respectively, such that  ${}^I\boldsymbol{\omega}_E = \mathbf{R}(t)\boldsymbol{\omega}_E(t)$  and, in particular,

$$\mathbf{m}(t) = \mathbf{R}^T(t){}^I\mathbf{m}, \quad (3)$$

for all  $t \geq 0$ . For ease of notation, the upper left superscripts of body vectors were dropped, hence  $\boldsymbol{\omega}_E \equiv {}^B\boldsymbol{\omega}_E$ .

From (2), the continuous matrix differential equation (1) can be rewritten as  $\dot{\mathbf{R}}(t) = \mathbf{R}(t)\mathbf{S}[\boldsymbol{\omega}_m(t) - \boldsymbol{\omega}_E(t)]$ .

The following assumptions are considered throughout the remainder of this letter.

*Assumption 1:* The constant inertial vectors  ${}^I\boldsymbol{\omega}_E$  and  ${}^I\mathbf{m}$  are not collinear, i.e.,  ${}^I\boldsymbol{\omega}_E \times {}^I\mathbf{m} \neq \mathbf{0}$ .

This assumption concerns observability purposes and will be fundamental in the main result of this letter. It is easily attainable in practice, as both vectors depend solely on the selected geographical location. In particular, it ensures that one can extract unequivocal information on directionality from the two vectors involved as long as they define a plane.

*Assumption 2:* The rate gyro measurements are bounded for all time, i.e., there exists  $\sigma > 0$  such that, for all  $t \geq 0$ ,  $\|\boldsymbol{\omega}_m(t)\| \leq \sigma$ .

This practical assumption is verified across all rate gyro devices since angular velocity readings cannot grow unbounded.

Consider now the following observer for the rotation matrix:

$$\dot{\hat{\mathbf{R}}}(t) = \hat{\mathbf{R}}(t)\mathbf{S}[\boldsymbol{\omega}_m(t) - \hat{\mathbf{R}}^T(t){}^I\boldsymbol{\omega}_E + \alpha\mathbf{m}(t) \times (\hat{\mathbf{R}}^T(t){}^I\mathbf{m})], \quad (4)$$

with  $\alpha > 0$ . Define also the error variable

$$\tilde{\mathbf{R}}(t) := \mathbf{R}(t)\hat{\mathbf{R}}^T(t) \in SO(3), \quad (5)$$

whose dynamics are given by  $\dot{\tilde{\mathbf{R}}}(t) = \dot{\mathbf{R}}(t)\hat{\mathbf{R}}^T(t) + \mathbf{R}(t)\dot{\hat{\mathbf{R}}}^T(t) = \mathbf{R}(t)\mathbf{S}[\boldsymbol{\omega}_m(t) - \boldsymbol{\omega}_E(t)]\hat{\mathbf{R}}^T(t) - \mathbf{R}(t)\mathbf{S}[\boldsymbol{\omega}_m(t) - \hat{\mathbf{R}}^T(t){}^I\boldsymbol{\omega}_E + \alpha\mathbf{m}(t) \times (\hat{\mathbf{R}}^T(t){}^I\mathbf{m})]\hat{\mathbf{R}}^T(t)$ . Isolating the terms associated with the Earth's angular velocity, and further noticing that the terms corresponding to the measurements of angular velocity cancel each other, allows to write  $\dot{\tilde{\mathbf{R}}}(t) = -\mathbf{R}(t)\mathbf{S}[(\mathbf{R}^T(t) - \hat{\mathbf{R}}^T(t)){}^I\boldsymbol{\omega}_E]\hat{\mathbf{R}}^T(t) - \mathbf{R}(t)\mathbf{S}[\alpha(\mathbf{R}^T(t){}^I\mathbf{m}) \times (\hat{\mathbf{R}}^T(t){}^I\mathbf{m})]\hat{\mathbf{R}}^T(t)$ . Since  $\mathbf{R}^T(t)\mathbf{R}(t) = \mathbf{I}$ , the previous result can be rewritten as

$$\begin{aligned} \dot{\tilde{\mathbf{R}}}(t) = & -\mathbf{R}(t)\mathbf{S}[(\mathbf{R}^T(t) - \hat{\mathbf{R}}^T(t)){}^I\boldsymbol{\omega}_E]\mathbf{R}^T(t)\mathbf{R}(t)\hat{\mathbf{R}}^T(t) + \\ & -\mathbf{R}(t)\mathbf{S}[\alpha(\mathbf{R}^T(t){}^I\mathbf{m}) \times (\hat{\mathbf{R}}^T(t){}^I\mathbf{m})]\mathbf{R}^T(t)\mathbf{R}(t)\hat{\mathbf{R}}^T(t). \end{aligned} \quad (6)$$

Recall the error definition in (5), and employ the property  $\mathbf{R}(t)\mathbf{S}[\mathbf{a}]\mathbf{R}^T(t) = \mathbf{S}[\mathbf{R}(t)\mathbf{a}]$ ,  $\mathbf{a} \in \mathbb{R}^3$ , to help simplifying (6) as  $\dot{\tilde{\mathbf{R}}}(t) = -\mathbf{S}[(\mathbf{R}(t)\mathbf{R}^T(t) - \mathbf{R}(t)\hat{\mathbf{R}}^T(t)){}^I\boldsymbol{\omega}_E]\tilde{\mathbf{R}}(t) - \mathbf{S}[\mathbf{R}(t)\alpha(\mathbf{R}^T(t){}^I\mathbf{m}) \times (\hat{\mathbf{R}}^T(t){}^I\mathbf{m})]\tilde{\mathbf{R}}(t)$ . Finally, rearrange to

obtain the autonomous system

$$\begin{aligned} \dot{\tilde{\mathbf{R}}}(t) = & -\mathbf{S}\left[(\mathbf{I} - \tilde{\mathbf{R}}(t)){}^I\boldsymbol{\omega}_E + \tilde{\mathbf{R}}(t)\alpha(\tilde{\mathbf{R}}^T(t){}^I\mathbf{m}) \times {}^I\mathbf{m}\right]\tilde{\mathbf{R}}(t) \\ = & \tilde{\mathbf{R}}(t)\mathbf{S}\left[(\mathbf{I} - \tilde{\mathbf{R}}^T(t)){}^I\boldsymbol{\omega}_E - \alpha(\tilde{\mathbf{R}}^T(t){}^I\mathbf{m}) \times {}^I\mathbf{m}\right]. \end{aligned} \quad (7)$$

This last result poses a highly nonlinear relationship, whereby classical tools from the linear system theory cannot be applied. However, the angle-axis representation of the nonlinear error dynamics (7) proves extremely convenient, as attested by the stability analysis conducted in the next section of this letter, where any positive gain  $\alpha$  is shown to drive the observer error to zero, i.e., drive the error matrix  $\tilde{\mathbf{R}}(t)$  to an identity, according to (5).

### III. MAIN RESULT OF THIS LETTER

Start by defining the domain  $D := [0, \pi]$ , and consider the Euler angle-axis representation of the error associated with the rotation matrix,

$$\tilde{\mathbf{R}}(t) = \mathbf{I} + \sin(\tilde{\theta}(t))\mathbf{S}[\tilde{\mathbf{v}}(t)] + [1 - \cos(\tilde{\theta}(t))]\mathbf{S}^2[\tilde{\mathbf{v}}(t)], \quad (8)$$

where  $\tilde{\theta}(t) \in D$  and  $\tilde{\mathbf{v}}(t) \in S(2)$  form the Euler angle-axis pair. In the sequel, consider as well the square of (8), which also consists in a rotation matrix, and is given by

$$\tilde{\mathbf{R}}^2(t) = \mathbf{I} + \sin(2\tilde{\theta}(t))\mathbf{S}[\tilde{\mathbf{v}}(t)] + 2\sin^2(\tilde{\theta}(t))\mathbf{S}^2[\tilde{\mathbf{v}}(t)]. \quad (9)$$

The following theorem is the main result of this letter.

*Theorem 1:* Consider the attitude observer (4), along with the error definition (5) and the set of measurements including body-fixed readings of both the angular velocity, as given by (2), and the constant inertial reference vector, as given by (3). Further suppose that both assumptions 1 and 2 are verified and define the set  $\Omega \subset SO(3)$  as  $\Omega = \{\tilde{\mathbf{R}}(t) \mid \text{tr}(\tilde{\mathbf{R}}(t)) = -1\}$ . Then: i) the set  $\Omega$  is forward invariant and unstable with respect to the observer dynamics (4); and, ii) the rotation matrix error  $\tilde{\mathbf{R}}(t)$  converges locally exponentially fast to  $\mathbf{I}$ , and is AGAS to  $\mathbf{I}$  as well.

*Proof:* Let  $V : D \rightarrow \mathbb{R}$  be a positive bounded Lyapunov-like candidate function given by  $V(\tilde{\theta}(t)) = 1 - \cos(\tilde{\theta}(t)) = \frac{1}{2}\text{tr}(\mathbf{I} - \tilde{\mathbf{R}}(t))$ . The derivative of  $V(\tilde{\theta}(t))$  results in

$$\dot{V} = -\frac{1}{2}\text{tr}(\dot{\tilde{\mathbf{R}}}(t)). \quad (10)$$

Substituting (7) in (10) and noticing that  $\text{tr}(\tilde{\mathbf{R}}(t)\mathbf{S}[(\mathbf{I} - \tilde{\mathbf{R}}^T(t)){}^I\boldsymbol{\omega}_E]) = 0$  allows to rewrite (10) as

$$\dot{V} = \frac{\alpha}{2}\text{tr}(\tilde{\mathbf{R}}(t)\mathbf{S}[(\tilde{\mathbf{R}}^T(t){}^I\mathbf{m}) \times {}^I\mathbf{m}]). \quad (11)$$

Now, since  $(\tilde{\mathbf{R}}^T(t){}^I\mathbf{m}) \times {}^I\mathbf{m} = \mathbf{S}[\tilde{\mathbf{R}}^T(t){}^I\mathbf{m}]{}^I\mathbf{m}$ , the cross-product property  $\mathbf{S}[\mathbf{S}[\mathbf{a}]\mathbf{b}] = \mathbf{b}\mathbf{a}^T - \mathbf{a}\mathbf{b}^T$  helps to simplify (11) as

$$\dot{V} = -\frac{\alpha}{2}\|{}^I\mathbf{m}\|^2 + \frac{\alpha}{2}\text{tr}({}^I\mathbf{m}{}^I\mathbf{m}^T\tilde{\mathbf{R}}^2(t)), \quad (12)$$

where a few related properties were employed. Next, substitute (9) in (12), and further simplify in order to obtain

$$\begin{aligned} \dot{V} = & \alpha\sin^2(\tilde{\theta}(t))\text{tr}({}^I\mathbf{m}{}^I\mathbf{m}^T\mathbf{S}^2[\tilde{\mathbf{v}}(t)]) \\ & + \frac{\alpha}{2}\sin(2\tilde{\theta}(t))\text{tr}({}^I\mathbf{m}{}^I\mathbf{m}^T\mathbf{S}[\tilde{\mathbf{v}}(t)]). \end{aligned} \quad (13)$$

Since  ${}^I\mathbf{m}\mathbf{m}^T$  is symmetric and  $\mathbf{S}[\tilde{\mathbf{v}}(t)]$  is skew-symmetric, it follows that  $\text{tr}({}^I\mathbf{m}\mathbf{m}^T\mathbf{S}[\tilde{\mathbf{v}}(t)]) = 0$ . Furthermore, given that  $\mathbf{S}^2[\tilde{\mathbf{v}}(t)] = \tilde{\mathbf{v}}(t)\tilde{\mathbf{v}}^T(t) - \mathbf{I}$ , the result in (13) can be written as  $\dot{V} = \alpha \sin^2(\tilde{\theta}(t))[({}^I\mathbf{m}^T\tilde{\mathbf{v}}(t))^2 - \|{}^I\mathbf{m}\|^2] \leq 0$ . Hence, equation  $\dot{V} = 0$  is satisfied on three occasions, when: 1)  $\tilde{\theta}(t) = \pi$ , which, according to (8), corresponds to the condition  $\text{tr}(\tilde{\mathbf{R}}(t)) = -1$ , with  $\tilde{\mathbf{R}}(t) = \tilde{\mathbf{R}}^T(t)$ ; 2)  $\tilde{\theta}(t) = 0$ , which means  $\tilde{\mathbf{R}}(t) = \mathbf{I}$ ; or 3)  $\tilde{\mathbf{v}}(t) = \pm {}^I\mathbf{m}/\|{}^I\mathbf{m}\|$ , which implies either that  $\tilde{\mathbf{R}}(t){}^I\mathbf{m} = {}^I\mathbf{m}$  or  $\tilde{\mathbf{R}}^T(t){}^I\mathbf{m} = {}^I\mathbf{m}$ . Notice first that system trajectories associated with the third case are not invariant in the sense that they do not correspond to an equilibrium point of the error dynamics (7). Indeed, the latter can be written as  $\dot{\tilde{\mathbf{R}}}(t) = \tilde{\mathbf{R}}(t)\mathbf{S}[\omega_E] - \mathbf{S}[\omega_E]\tilde{\mathbf{R}}(t)$ , which, according to (8), and by using  $\tilde{\mathbf{v}}(t) = \pm {}^I\mathbf{m}/\|{}^I\mathbf{m}\|$ , is equivalent to  $\dot{\tilde{\mathbf{R}}}(t) = \pm \sin\tilde{\theta}(t) \mathbf{S}[{}^I\mathbf{m} \times {}^I\omega_E]/\|{}^I\mathbf{m}\| \pm (1 - \cos(\tilde{\theta}(t))) \mathbf{S}[({}^I\omega_E \times {}^I\mathbf{m}) \times {}^I\mathbf{m}]/\|{}^I\mathbf{m}\|^2$ . Therefore, since Assumption 1 holds, and since  ${}^I\mathbf{m} \times {}^I\omega_E$  is orthogonal to  $({}^I\omega_E \times {}^I\mathbf{m}) \times {}^I\mathbf{m}$ , it follows that  $\dot{\tilde{\mathbf{R}}}(t) \neq \mathbf{0}$ .

The next steps consists in showing that the set  $\Omega$  is indeed forward invariant with respect to the error dynamics (7). The derivative of  $\text{tr}(\tilde{\mathbf{R}}(t))$  can be computed as  $\frac{d}{dt}\text{tr}(\tilde{\mathbf{R}}(t)) = \text{tr}(\dot{\tilde{\mathbf{R}}}(t)) = \text{tr}(\tilde{\mathbf{R}}(t)\mathbf{S}[\omega_E] - \mathbf{S}[\omega_E]\tilde{\mathbf{R}}(t)) = 0$ , which asserts forward invariance of the set  $\Omega$ . Accordingly, by applying LaSalle's principle to the solutions of the proposed observer dynamics (4), one concludes that  $\tilde{\mathbf{R}}(t)$  converges asymptotically to either  $\mathbf{I}$  or some rotation matrix belonging to  $\Omega$ .

In [17], local exponential stability of the isolated equilibrium point  $\mathbf{I}$  was shown through the linearization of the rotation error dynamics (7), thus proving the theorem's statement ii). The companion step consists in showing that the set  $\Omega$  is unstable, which shall be done resorting to the quaternion representation of the rotation matrix error (see the Appendix), as given by (15). According to this quaternion formulation, the forward invariant set  $\Omega$  associated with the rotation error dynamics (7) is described by  $\Omega = \{(\tilde{s}, \tilde{\mathbf{r}}) \mid \tilde{s} = 0, \tilde{\mathbf{r}}^T\tilde{\mathbf{r}} = 1\}$ . Then, from (17), the dynamics of  $\tilde{s}(t)$  follows as  $\dot{\tilde{s}}(t) = \alpha[\|{}^I\mathbf{m}\|^2\|\tilde{\mathbf{r}}(t)\|^2 - ({}^I\mathbf{m}^T\tilde{\mathbf{r}}(t))^2]\tilde{s}(t)$ , which is clearly unstable for any point  $\tilde{s} \neq 0$ , given that, based on (16),  $\frac{d}{dt}{}^I\mathbf{m}^T\tilde{\mathbf{r}}(t) = {}^I\mathbf{m}^T\dot{\tilde{\mathbf{r}}}(t) = -{}^I\mathbf{m}^T\mathbf{S}[\omega_E]\tilde{\mathbf{r}}(t) + \alpha({}^I\mathbf{m}^T\tilde{\mathbf{r}}(t))\|{}^I\mathbf{m} \times \tilde{\mathbf{r}}(t)\|^2$ , which, in view of Assumption 1 can never be identically zero. Therefore,  $\tilde{s}(t)$  is a strictly increasing function for all  $t \geq 0$ , which means set  $\Omega$  corresponds to an unstable equilibrium point. This proves the theorem's statement i) and thus the overall proof is complete. ■

*Remark 1:* Despite stability guarantees, the rate of convergence of the observer has not been properly addressed. In fact, unless one solves the nonlinear equation (7), to infer something about this rate is an extremely intricate exercise.

#### IV. SIMULATION RESULTS

In this section, a realistic scenario is simulated within the scope of attitude estimation of robotic platforms when high accuracy is a crucial demand. This typically concerns either smooth vehicle trajectories, where accelerations clearly are dominated by the gravitational field and where magnetometer readings can be heavily corrupted by hard- and soft-iron

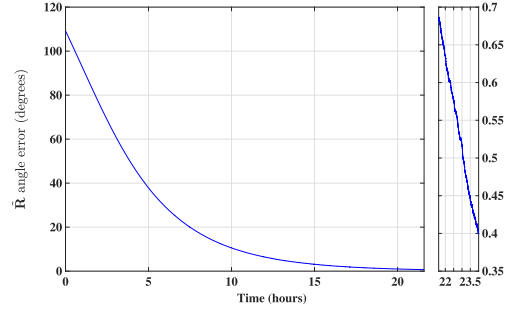


Fig. 1. Angle error evolution for  $\tilde{\theta}(0) \approx 109.2$  degrees.

effects, or mission scenarios involving quick maneuvers that give rise to high vehicle accelerations, but where measurements of the magnetic field are highly reliable.

Start by considering a robotic platform describing a rotational motion in a three-dimensional space, located at a latitude of  $\varphi = 38.777816^\circ$ , a longitude of  $\psi = 9.097570^\circ$ , and at sea level. Taking into account the length of time known as sidereal day, the corresponding norm of the Earth's angular velocity is approximately  $\|{}^I\omega_E\| = 7.2921159 \times 10^{-5}$  rad/s, while its vectorial representation in the North-East-Down (NED) frame is given by  ${}^I\omega_E = \|{}^I\omega_E\|[\cos(\varphi) \ 0 \ \sin(\varphi)]^T$  rad/s. Moreover, in light of the sea level and of the latitude and longitude indicated above, and according to the 12<sup>th</sup> generation of the International Geomagnetic Reference Field model, the components of the inertial magnetic field are given by  ${}^I\mathbf{m} = [26505.6 \ 1092.9 \ 34864.0]^T$  nT. As such, one easily asserts that  ${}^I\omega_E \times {}^I\mathbf{m} \neq \mathbf{0}$ , which satisfies Assumption 1. The angular velocity of the platform was designed to evolve according to  $\omega(t) = \frac{\pi}{180}[5 \sin(6\frac{\pi}{180}t), \sin(\frac{\pi}{180}t), -2 \sin(\frac{6}{5}\frac{\pi}{180}t)]$  (rad/s). Consider now that the robotic platform is equipped with the commercial off the shelf high-performance FOG IMU KVH DSP-1775, featuring an integrated three-axis magnetometer that provides magnetic field sensing. To emulate this sensor's worst specifications, a zero-mean white Gaussian noise sequence with standard deviation of 200 nT was added in simulation over the device measurements. According to the manufacturer, the FOG's digital data output is corrupted by an Angle Random Walk noise of  $0.7^\circ/\text{hr}/\sqrt{\text{Hz}}$ .

A sampling frequency of 100 Hz was considered and the fourth-order Runge-Kutta method was employed in all simulations. Finally, the scalar gain was set, after an empirical tuning process, to  $\alpha = 1.5 \times 10^{-4}/\|{}^I\mathbf{m}\|^2$ . This value is associated with the overall best performance that was attained, in general, given any possible initial condition.

##### A. Single Practical Example

Resorting to Euler angles to describe the orientation of the platform, its initial attitude was set to 150,  $-90$ , and 140 degrees of yaw, pitch and roll, respectively. The initial attitude estimate of the platform was set as  $\hat{\mathbf{R}}(0) = \mathbf{I}$ . In terms of the angle-axis representation expressed by (8), it follows  $\tilde{\theta}(0) \approx 109.2$  degrees.

The 24-hour evolution of the angle error is shown in Fig. 1. As seen from the main plot, despite the time window being insufficient to allow the estimator to enter steady-state, after

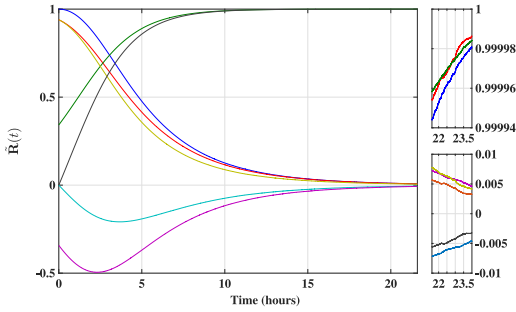


Fig. 2. Evolution of  $\tilde{\mathbf{R}}$  entries for  $\tilde{\theta}(0) \approx 109.2$  degrees. Upper right corner: diagonal entries of  $\tilde{\mathbf{R}}$ .

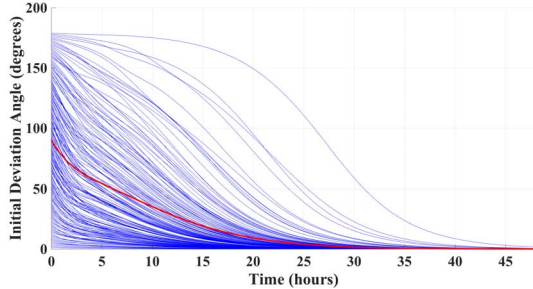


Fig. 3. Angle error evolution for  $\tilde{\theta}(0) = 1, 2, \dots, 179$ . Mean error evolution marked with thick red color.

roughly 15 hours the angle error is already below 5 degrees, a correction of over 100 degrees from the original deviation. In turn, the zoomed-in plot shows that, for  $t > 22$  h, the deviation is still converging and moving towards values below 0.4 degrees, which hints at a good overall performance for this kind of application. It is important to stress out that this level of convergence time is typical for space applications, where very high accuracy is required. For the sake of completeness, the corresponding evolution of the entries associated with the rotation matrix error is displayed in Fig. 2. Recall that this matrix, according to the error definition (5), evolves on the 2-sphere manifold, thus preserving the topological structure, even in the presence of noise.

### B. Monte Carlo Statistical Analysis

In order to assess the overall robustness of the proposed nonlinear observer, a Monte Carlo analysis was conducted. In terms of the angle-axis representation (8), for every initial angle error  $\tilde{\theta}(0) \in \{1, 2, \dots, 179\}$ , 10 runs were performed, each featuring: i) an initial axis error  $\tilde{\mathbf{v}}(0)$  generated from a sequence of normally distributed random numbers; and, ii) randomly generated additive white Gaussian noise sequences. Each 10 runs corresponding to the same initial angle deviation were then averaged, with the final result shown in Fig. 3. The mean error evolution, computed by averaging these resulting 179 convergent sequences, was also computed and is marked in red. As naturally expected, larger initial angle deviations correspond typically to longer convergence times, although the initial axis deviation also has some influence during the transient evolution, as noticeable from a few intersecting lines.

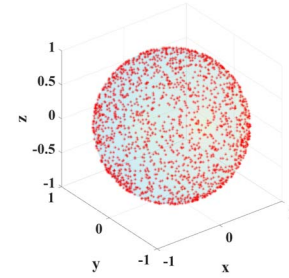


Fig. 4. Set of 1790 axis initializations on 3D unit sphere.

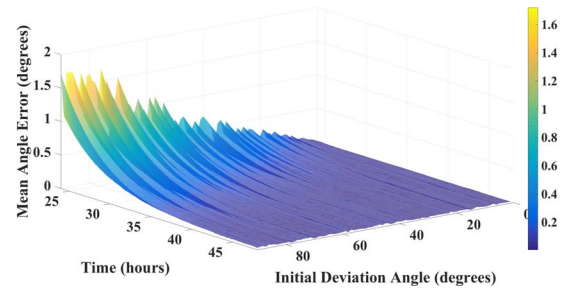


Fig. 5. Mean angle error in function of time ( $t > 24$ h) and initial angle error  $\tilde{\theta}(0)$ .

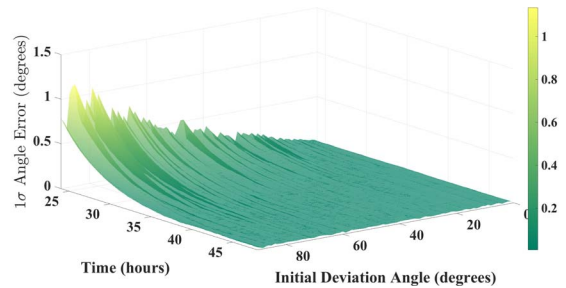


Fig. 6.  $1\sigma$  of angle error in function of time ( $t > 24$ h) and initial angle error  $\tilde{\theta}(0)$ .

Furthermore, Fig. 4 illustrates the set of initial axis deviations covering the unit sphere, demonstrating that the nonlinear observer was properly tested for (almost) all admissible initial conditions. The evolution over time of the mean and standard deviation associated with  $\tilde{\theta}(t)$ , for  $t > 24$  h and  $\tilde{\theta}(0) < 90$  degrees, are shown in Figs. 5 and 6, respectively. At  $t = 48$  h, both the mean and standard deviation were averaged across the 90 different sequences of  $\tilde{\theta}(t)$ . The final results yielded 0.0279 degrees and 0.008 degrees for mean and standard deviation, respectively, which are very good results for high-grate attitude determination systems.

In the context of attitude estimation in  $SO(3)$ , there exist alternative deterministic methods to design observers based on optimality criteria, for instance, the minimum-energy approach, as seen from [18], where an optimal attitude solution is obtained from minimizing a cost function. Herein the performance evaluation and observer parameter tuning is based on a Monte Carlo statistical analysis.

On a final note, in spite of the slow convergence times, it is important to stress out how extremely useful these results are

when no knowledge whatsoever about the initial orientation is available, i.e., when the initial error may be very large.

## V. CONCLUSION

In this letter, a nonlinear attitude observer built on  $SO(3)$  was proposed that takes into account the Earth's rotation and resorts exclusively to measurements of one constant inertial vector, in addition to angular velocity readings. Besides guarantees of local exponential stability, the proposed attitude estimation solution was also shown to be AGAS. Despite its slow convergence rates, this kind of observer is compatible with high-grade attitude determination systems, which take a long time to converge but exhibit a very good performance in terms of accuracy. Possible directions for future work will be along a performance and stability analysis when the reference vector is time-varying.

## APPENDIX

### UNIT QUATERNION REPRESENTATION

Let  $\mathbf{q}(t) \in \mathcal{Q}$  denote a unit quaternion with real and imaginary parts expressed by  $\tilde{s}(t) \in \mathbb{R}$  and  $\tilde{\mathbf{r}}(t) \in \mathbb{R}^3$ , respectively, with the group of unit quaternions being defined as  $\mathcal{Q} := \{\mathbf{q} = [\tilde{s} \ \tilde{\mathbf{r}}^T]^T \mid \mathbf{q}^T \mathbf{q} = 1\}$ . Take now the representation of  $\tilde{\mathbf{R}}(t)$  by means of the unit quaternion, which, in view of the angle-axis representation in (8), is given by

$$\tilde{\mathbf{R}}(t) = \mathbf{I} + 2\tilde{s}(t)\mathbf{S}[\tilde{\mathbf{r}}(t)] + 2\mathbf{S}^2[\tilde{\mathbf{r}}(t)], \quad (14)$$

where  $\tilde{s}(t) = \cos(\tilde{\theta}(t)/2)$  and  $\tilde{\mathbf{r}}(t) = \tilde{\mathbf{v}}(t) \sin(\tilde{\theta}(t)/2)$ . Next, recall the expression for the derivative of  $\tilde{\mathbf{R}}(t)$ , as expressed by (7), and write it as  $\dot{\tilde{\mathbf{R}}}(t) = \dot{\tilde{\mathbf{R}}}(t)\mathbf{S}[\tilde{\boldsymbol{\omega}}(t)]$ , with  $\tilde{\boldsymbol{\omega}}(t) := (\mathbf{I} - \tilde{\mathbf{R}}^T(t))^l \boldsymbol{\omega}_E - \alpha(\tilde{\mathbf{R}}^T(t)^l \mathbf{m}) \times {}^l \mathbf{m}$ . From this point, it is a simple matter of algebraic manipulations to show that the dynamics of  $\mathbf{q}(t)$  is given, in vector form, by

$$\begin{cases} \dot{\tilde{s}}(t) = -\frac{1}{2}\tilde{\mathbf{r}}^T(t)\tilde{\boldsymbol{\omega}}(t) \\ \dot{\tilde{\mathbf{r}}}(t) = \frac{1}{2}(\tilde{s}(t)\mathbf{I} + \mathbf{S}[\tilde{\mathbf{r}}(t)])\tilde{\boldsymbol{\omega}}(t). \end{cases} \quad (15)$$

Notice that, from (14), one can write  $(\tilde{\mathbf{R}}^T(t)^l \mathbf{m}) \times {}^l \mathbf{m} = \mathbf{S}[\tilde{\mathbf{R}}^T(t)^l \mathbf{m}]^l \mathbf{m} = -2({}^l \mathbf{m}^T \tilde{\mathbf{r}}(t))(\tilde{s}(t)\mathbf{I} - \mathbf{S}[\tilde{\mathbf{r}}(t)])^l \mathbf{m} + 2\tilde{s}(t)\|{}^l \mathbf{m}\|^2 \tilde{\mathbf{r}}(t)$ , where a few properties related to the cross product were employed. Further notice the equality  $\tilde{\mathbf{R}}(t)\tilde{\mathbf{r}}(t) = \tilde{\mathbf{r}}(t)$ . Moreover,  $(\mathbf{I} - \tilde{\mathbf{R}}^T(t))^l \boldsymbol{\omega}_E = 2(\tilde{s}(t)\mathbf{I} - \mathbf{S}[\tilde{\mathbf{r}}(t)])\mathbf{S}[\tilde{\mathbf{r}}(t)]^l \boldsymbol{\omega}_E$ , which, finally, allows to write  $\tilde{\boldsymbol{\omega}}(t) = 2(\tilde{s}(t)\mathbf{I} - \mathbf{S}[\tilde{\mathbf{r}}(t)])\mathbf{S}[\tilde{\mathbf{r}}(t)]^l \boldsymbol{\omega}_E - \alpha[-2({}^l \mathbf{m}^T \tilde{\mathbf{r}}(t))(\tilde{s}(t)\mathbf{I} - \mathbf{S}[\tilde{\mathbf{r}}(t)])^l \mathbf{m} + 2\tilde{s}(t)\|{}^l \mathbf{m}\|^2 \tilde{\mathbf{r}}(t)]$ . Substituting this in (15), the vector part of the quaternion dynamics follows as

$$\begin{aligned} \dot{\tilde{\mathbf{r}}}(t) = & \left(-\mathbf{S}^l[\boldsymbol{\omega}_E] + \alpha\mathbf{S}^2[{}^l \mathbf{m}]\right)\tilde{\mathbf{r}}(t) + \\ & -\alpha\|\tilde{\mathbf{r}}(t)\|^2\mathbf{S}^2[{}^l \mathbf{m}]\tilde{\mathbf{r}}(t) - \alpha({}^l \mathbf{m}^T \tilde{\mathbf{r}}(t))\mathbf{S}^2[\tilde{\mathbf{r}}(t)]^l \mathbf{m}. \end{aligned} \quad (16)$$

For the sake of completeness, the dynamics associated with  $\tilde{s}(t)$  follows as

$$\dot{\tilde{s}}(t) = \alpha \left[ \|{}^l \mathbf{m}\|^2 \|\tilde{\mathbf{r}}(t)\|^2 - ({}^l \mathbf{m}^T \tilde{\mathbf{r}}(t))^2 \right] \tilde{s}(t). \quad (17)$$

*Remark 2:* The 1st-order approximation of the nonlinear differential equation (16) yields a linear time-invariant (LTI) system that can be expressed by  $\dot{\mathbf{z}}(t) = (-\mathbf{S}^l[\boldsymbol{\omega}_E] + \alpha\mathbf{S}^2[{}^l \mathbf{m}])\mathbf{z}(t)$ . Notably, as shown in [17], the 1st-order approximation of (7) yields an identical LTI system, for which any scalar  $\alpha > 0$  was proved to render the nonlinear error dynamics locally exponentially stable.

## REFERENCES

- [1] G. Wahba, "A least squares estimate of satellite attitude," *SIAM Rev.*, vol. 7, no. 3, p. 409, 1965.
- [2] P. Martin and E. Salaün, "Design and implementation of a low-cost observer-based attitude heading reference system," *Control Eng. Pract.*, vol. 18, no. 7, pp. 712–722, Jul. 2010.
- [3] J. F. Vasconcelos, B. Carneira, C. Silvestre, P. Oliveira, and P. Batista, "Discrete-time complementary filters for attitude and position estimation: Design, analysis and experimental validation," *IEEE Trans. Control Syst. Technol.*, vol. 19, no. 1, pp. 181–198, Jan. 2011.
- [4] J. L. Crassidis, F. L. Markley, and Y. Cheng, "Survey of nonlinear attitude estimation methods," *J. Guid. Control Dyn.*, vol. 30, no. 1, pp. 12–28, Jan. 2007.
- [5] A. Barrau and S. Bonnabel, "The invariant extended Kalman filter as a stable observer," *IEEE Trans. Autom. Control*, vol. 62, no. 4, pp. 1797–1812, Apr. 2017.
- [6] R. Mahony, T. Hamel, and J.-M. Pfimlin, "Nonlinear complementary filters on the special orthogonal group," *IEEE Trans. Autom. Control*, vol. 53, no. 5, pp. 1203–1218, Jun. 2008.
- [7] F. L. Markley, "Attitude filtering on SO(3)," *J. Astronaut. Sci.*, vol. 54, no. 3, pp. 391–413, 2006.
- [8] P. Batista, C. Silvestre, and P. Oliveira, "Attitude and earth velocity estimation—Part II: Observer on the special orthogonal group," in *Proc. IEEE 53rd Annu. Conf. Decis. Control (CDC)*, Los Angeles, CA, USA, 2014, pp. 127–132.
- [9] D. S. Laila, M. Lovera, and A. Astolfi, "A discrete-time observer design for spacecraft attitude determination using an orthogonality-preserving algorithm," *Automatica*, vol. 47, no. 5, pp. 975–980, May 2011.
- [10] P. Batista, C. Silvestre, and P. Oliveira, "Attitude and earth velocity estimation—Part I: Globally exponentially stable observer," in *Proc. IEEE 53rd Annu. Conf. Decis. Control (CDC)*, Los Angeles, CA, USA, 2014, pp. 121–126.
- [11] S. P. Bhat and D. S. Bernstein, "A topological obstruction to continuous global stabilization of rotational motion and the unwinding phenomenon," *Syst. Control Lett.*, vol. 39, no. 1, pp. 63–70, Jan. 2000.
- [12] U. V. Kalabić, R. Gupta, S. Di Cairano, A. M. Bloch, and I. V. Kolmanovskiy, "MPC on manifolds with an application to the control of spacecraft attitude on SO(3)," *Automatica*, vol. 76, pp. 293–300, Feb. 2017.
- [13] S. Berkane, A. Abdessameud, and A. Tayebi, "Hybrid attitude and gyro-bias observer design on SO(3)," *IEEE Trans. Autom. Control*, vol. 62, no. 11, pp. 6044–6050, Nov. 2017.
- [14] S. Bahrani and M. Namvar, "Global attitude estimation using single delayed vector measurement and biased gyro," *Automatica*, vol. 75, pp. 88–95, Jan. 2017.
- [15] A. Barrau and S. Bonnabel, "Intrinsic filtering on lie groups with applications to attitude estimation," *IEEE Trans. Autom. Control*, vol. 60, no. 2, pp. 436–449, Feb. 2015.
- [16] W. Sun, A.-G. Xu, and Y. Gao, "Strapdown gyrocompass algorithm for AUV attitude determination using a digital filter," *Measurement*, vol. 46, no. 1, pp. 815–822, Jan. 2013.
- [17] J. Reis, P. Batista, P. Oliveira, and C. Silvestre, "Nonlinear attitude observer on SO(3) based on single body-vector measurements," in *Proc. 2nd IEEE Conf. Control Technol. Appl.*, Copenhagen, Denmark, Aug. 2018, pp. 1319–1324.
- [18] M. Zamani, J. Trunpf, and R. Mahony, "Minimum-energy filtering for attitude estimation," *IEEE Trans. Autom. Control*, vol. 58, no. 11, pp. 2917–2921, Nov. 2013.